

Flexible Needle Steering and Optimal Trajectory Planning for Percutaneous Therapies

Daniel Glozman and Moshe Shoham

Medical Robotics Laboratory, Mechanical Engineering Department,
Technion – Israel Institute of Technology, Israel, 32000
{glozman, shoham}@technion.ac.il
<http://robotics.technion.ac.il>

Abstract. Flexible needle insertion into viscoelastic tissue is modeled in this paper with a linear beam supported by virtual springs. Using this simplified model, the forward and inverse kinematics of the needle is solved analytically, providing a way for simulation and path planning in real-time. Using the inverse kinematics, the required needle basis trajectory can be computed for any desired needle tip path. It is shown that the needle base trajectory is not unique and can be optimized to minimize lateral pressure of the needle body on the tissue. Experimental results are provided of robotically assisted insertion of flexible needle while avoiding “obstacle”.

1 Introduction

The current trend of contemporary medicine is less invasiveness and localized therapy. One of the most common procedures employed in modern clinical practice involves percutaneous insertion of needles and catheters for biopsy and drug delivery. Percutaneous procedures involving needle insertions include vaccinations, blood/fluid sampling, regional anesthesia, tissue biopsy, catheter insertion, cryogenic ablation, electrolytic ablation, brachytherapy, neurosurgery, deep brain stimulation, minimally invasive surgeries and more.

Complications are due, in large part, to poor technique and needle placement [1]. Physicians and surgeons often rely only upon kinesthetic feedback from the tool, correlated with their own mental 3-D visualization of anatomic structures. It was shown in [2], that as the needle penetrates the tissue, the tissue deforms and even straight needles miss the target. Thick and nonflexible needles are easily pointed to the target in the existence of visualization system, but their manipulation causes significant pressure on the tissue. Moreover, straight needles are not suitable for following curved paths, if obstacle avoidance is required.

These problems can be solved by introducing thin and flexible needles. Moreover, it is known that thinner needles cause less pain to the patient. On the other hand, flexible needle navigation deep inside the tissue is very complicated. The system has non-minimum phase behavior and does not lend itself to intuitive control. Path planning for flexible needle insertion and obstacles avoidance inside the body tissue is a challenging problem of mechanics and robotics. Creating an automated system that

can plan and perform thin, flexible needle insertion will minimize misplacements, and reduce both risks and patient suffering.

Needle insertion causes the surrounding soft tissues to displace and deform. DiMaio *et al.* used finite elements simulation for determining such displacements [2]. Using this approach, Alteroviz *et al.* suggest a way to predict needle placement error in prostate brachytherapy procedure and to correct for this error by choosing an appropriate straight needle insertion point [4]. Because of its complexity, the method does not allow online correction of the placement error.

Current methods and techniques all use straight, rigid needles since they are easier to control and their trajectory is well defined. On the other hand, it is known that thinner needles cause less damage and reduce post puncture outcome, as in Post Dural Puncture Headache (PDPH) appearing after spinal anesthesia. As a general rule, the relative risk of PDPH decreases with each successive reduction in needle diameter [5]. Thinner needles are more flexible and thus results in less pressure and damage to the tissue. They allow making curved trajectories and accomplishing easier obstacle avoidance. They are, however, very difficult to control.

An active, flexible steering system using shape memory alloys has been suggested in [6] for a steering catheter. Such a system is not suitable for thin needle navigation because of size limitations. Kataoka *et al.* investigated needle deflection due to the bevel of the tip during linear needle insertion and expressed the deflection as function of driving force [7].

Flexible needle steering was first addressed by DiMaio *et al.* [3]. To solve the inverse kinematics of the needle, iterative numerical computing of the flexible needle's Jacobian is suggested. The computation involves solving for two-dimensional finite element mesh of the tissue and iterative nonlinear flexion of a beam and requires nine independent computations for devising the Jacobian elements. The computation complexity does not allow real-time simulation and control of the system.

The present investigation suggests a simplified model that allows fast path planning and real time tracking for the needle insertion procedure. The future goal of this work is the creation of an image based closed loop system for automatic flexible needle insertion. The concept is described in 2-D space.

2 The Virtual Springs Model

Modeling of a flexible needle is based in this investigation on the assumption of quasistatic motion, so the needle is in equilibrium state at each step. It is known that biologic soft tissue deflection is nonlinear with strain, but for small displacements, locally, we can assume linear lateral force response, based on the work of Simone *et al.* [8] and [9]. The tissue forces on the needle are modeled as lateral virtual springs distributed along the needle curve plus friction forces tangent to the needle. Since the tissue elastic modulus differs as a function of strain, we update the virtual spring's coefficients according to the elastic modulus corresponding to the current strain, and linearize the system at each step. The concept is illustrated in Figure 1.

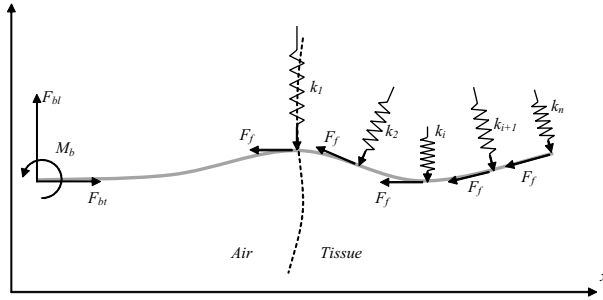


Fig. 1. Virtual springs model: the tissue's reaction is modeled by distributed virtual springs.

As the shape of the needle changes, the location and orientation of the virtual springs change as well. Locally, at each step, the linearized system model yields the shape of the needle at this step. There is no physical meaning for the free length of the virtual springs, and the only important parameter of the spring is the local stiffness coefficient, which expresses the force of the tissue on the needle as a function of local displacement. The stiffness coefficients of the virtual springs are determined either experimentally or by using preoperative images by assuming empiric values for known tissues and organs.

The Linearized System Solution

Initially, assuming small displacements, we approximate the needle by a linear beam subjected to point forces as shown on Figure 2. With appropriate elements spacing, this approximation is close to the flexible beam on elastic foundation model.

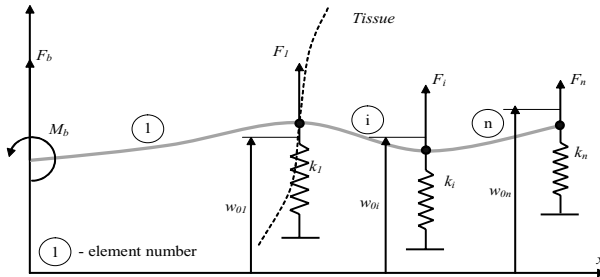


Fig. 2. Linear system model. Flexible beam subjected to a number of virtual springs.

At each joint, the force applied by the virtual spring is proportional to the spring's displacement from its initial position:

$$F_i = k_i (w_i - w_{0i}) \quad (1)$$

where k_i is the virtual spring coefficient, w_i - displacement at point i , and w_{0i} - is the position of freed spring i .

Since the forces are a function of the deflection, this problem cannot be solved by superposition. It can be solved only globally for all the elements of the beam. We define each element as the part of the beam between two neighboring forces. Thus the first element is the part of the needle outside of the tissue, and the rest of the elements are distributed along the inner part according to the level of discretization. Each element behaves as a linear beam subjected to shearing forces at its borders. Since we assume linear flexible beam, the displacement of each element is given by a third degree polynomial. We adopt the nodal degrees of freedom from finite elements theory, in which the coordinates are specifically identified with a single nodal point and represent a displacement or rotation, having clear physical interpretation. The displacement $y(x)$ will have the form of:

$$y(x) = N_1\phi_1 + N_2\phi_2 + N_3\phi_3 + N_4\phi_4 \quad (2)$$

N_1, N_3 are the coordinates and N_2, N_4 are the slopes at $x=0$ and $x=l$ of an element, respectively. ϕ_i are the shape functions of third degree.

Substituting boundary conditions as displacement and slope at the base and tip of the needle, the result is $4 \times n$ equations - 2 at each side and 4 for each internal node, which yields the global matrix equation:

$$[K]\bar{N} = \bar{Q} \quad (3)$$

where K is the matrix of coefficients of $N_{i,j}$ - elements degrees of freedom. N is the vector of $N_{i,j}$, where i is the number of the element and j is the number of degrees of freedom, Q are the free coefficients.

The 3 DOF Forward Kinematics

The above solution solves for the displacements and rotations of the needle for 2 DOF of needle base - vertical translation y and slope θ . But the main translation of the needle is in x - axial direction. Applying axial translation to the non-compressible needle means that the outside tissue part of the needle becomes shorter by the size of translation x . And an additional element of length x is added to the last element. Assuming that the last $(n+1)$ element is relatively small, and the forces on it create negligible moments, its shape is taken as a straight line, having the slope of the last element.

In summary, given 3 displacements of the 3 DOF of the needle's base, we are now able to calculate the 3 DOF translations of the needle tip, thus completing the forward kinematics solution.

The 3 DOF Inverse Kinematics

In an actual needle insertion problem, the essence is the trajectory following by the needle's tip. First, there is a need to hit the target with the tip; second, the obstacle organs should be avoided. This is the problem of inverse kinematics; namely, for given position and orientation of the tip, calculate the translation and orientation of the needle base.

Let us expand the matrix of equation (3):

$$\begin{bmatrix} 1 & 0 & \cdots & 0 & 0 \\ 0 & -1 & \cdots & 0 & 0 \\ \hline & \tilde{K}_{21} & & \tilde{K}_{22} & \end{bmatrix} \begin{pmatrix} N_{11} \\ N_{12} \\ \vdots \\ N_{n3} \\ N_{n4} \end{pmatrix} = \begin{pmatrix} Y \\ \theta \\ \vdots \\ \vdots \end{pmatrix} \quad (4)$$

In the forward kinematics, given the base translation Y and rotation θ , one can solve for $N_{i,j}$. Note that the last two elements of vector N are the translation and rotation of the tip. But in the inverse kinematics problem, the translation and rotation of the tip - N_{n3} , N_{n4} are known and the unknowns are the translation and rotation of the base - Y and θ or N_{11} and N_{12} . Since in the last two equations the two variables are known, we can write (4) as:

$$\begin{aligned} [\tilde{K}_{21}] \tilde{N} &= \tilde{Q} - \tilde{K}_{22} \begin{pmatrix} N_{n3} \\ N_{n4} \end{pmatrix} \\ Y &= N_{11} \\ \theta &= N_{12} \end{aligned} \quad (5)$$

where \tilde{N}, \tilde{Q} are the original vectors \bar{N}, \bar{Q} without the last two elements. \tilde{K}_{21} is (n-2)×(n-2) matrix and equation (5) can be solved for \tilde{N} and therefore for Y and θ , which is the solution of the inverse kinematics.

Path Planning

The simple linear path is straightforward. The main challenge is avoiding obstacles, while applying minimal pressure on the tissue, especially vital organs. In the presence of obstacles, the best path should require minimal curvature of the needle. The path planning problem thus reduces to finding the shortest curve, connecting the target and needle insertion point, and avoiding obstacles. It can either be defined by the algorithm or constrained by the doctor.

Trajectory Tracking and Optimization

Trajectory tracking problem means computation of the needle base position and orientation for a given tip trajectory. To solve this problem, full simulation of needle insertion is required, since every step is dependent on the previous history of insertion. Here we will concentrate on one tracking method - moving the tip from one given position and orientation to another position. As explained above, it is possible to reach the desired position with various tip orientations. Since in the needle insertion procedure, orientation of the tip is of less importance, one can reach the desired position with different allowed tip orientations to accomplish the task. For example we require

that the needle stay as straight as possible in order to keep minimal pressure on the tissue. The sum of the needle deflections is given by S :

$$S = \min \sum_{i=1}^n (w_i^2 + \theta_i^2) = \min \sum_{i=1}^n \sum_{j=1}^4 N_{ij}^2 \tag{6}$$

Nodes displacements are a function of desired tip orientation from (5). To get the minimum of S , we differentiate (6) for θ_i and equalize to zero:

$$\frac{dS}{d\theta_i} = \sum_{i=1}^n \sum_{j=1}^4 2N_{ij} \frac{dN_{ij}}{d\theta_i} = 0 \tag{7}$$

The slope of the last element N_{4n} is not known, hence there is one more unknown than equations. Instead, we add the minimization equation (7), so that the number of unknown variables equals the number of equations.

3 Needle Insertion Simulation

As the needle penetrates deeper into the tissue, additional virtual springs are introduced. The following example simulates needle tip sine wave tracking, thus avoiding an obstacle in the tissue. For simplicity, we draw the virtual springs as a compressible mesh below and above the needle, since the tissue is on both sides. The trajectory, where the tip is forced to be tangent to the trajectory is shown in Figure 3. An optimized for minimal tissue pressure trajectory is shown in Figure 4.

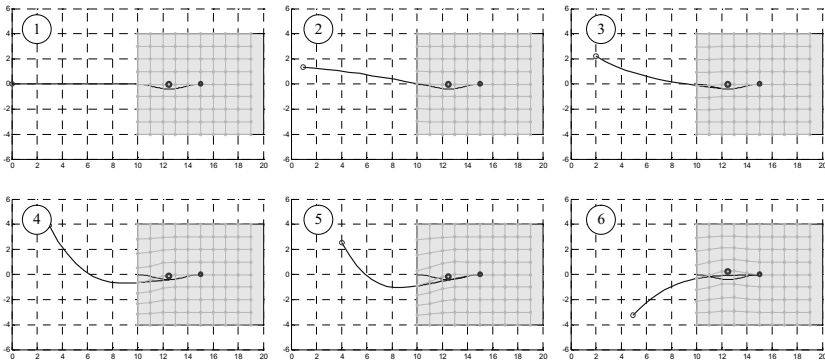


Fig. 3. Simulating needle insertion for tip oriented tangent to the path.

The simulation starts with one element beam of 100 mm length, at step 1. With each advancement of 10 mm into the tissue, the element is subdivided, adding a new element of 10 mm and a virtual spring at the tip of the needle. At the 6th step, there are 6 elements and 6 virtual springs.

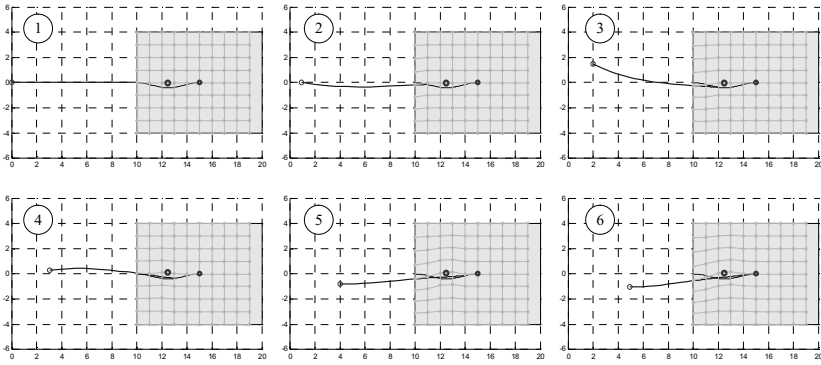


Fig. 4. Simulating needle insertion while minimizing pressure on the tissue.

4 Qualitative Experiment

We performed a qualitative experiment using the RSPR parallel robot [10] as shown in Figure 5. For the tissue we used chicken breast slice of 8mm thickness and the needle is a spinal 22G×90mm – outer diameter 0.711mm, connected through ATI Nano17 6DOF force sensor. With proper lighting it was possible to see through the tissue and to obtain images of reasonable quality. The tissue is placed in a 100mm×100mm frame and constrained in one plane between two glass plates. The stiffness coefficient of the virtual springs was experimentally evaluated by needle force measurement to 60 N/m.

Two metal pieces were inserted into the tissue prior to the experiment – one for the target and one for the obstacle. The robot was required to follow the path, computed with the above algorithm, avoiding the obstacle and hitting the target. The images corresponding to steps 1,3,4,6 of simulation shown in Figure 4 are shown in Figure 5. As can be observed, the path followed by the needle tip is similar to the preplanned.

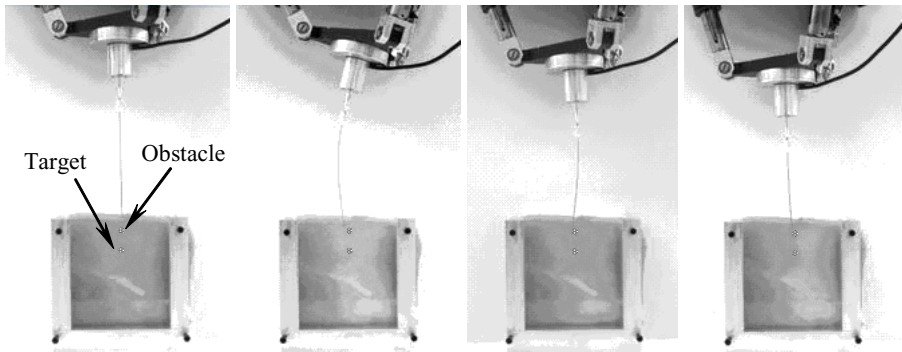


Fig. 5. Robotic needle insertion at simulation steps 1,3,4,6.

5 Conclusion

This investigation develops the planar linearized model approximation for the flexible needle insertion problem with small deflections. Using this model, the inverse and forward kinematics of needle insertion can be solved in one step, solving a low dimensional linear system of equations. Path planning and its optimization for minimal tissue pressure were developed. It was found that this model can be solved in a closed form for a given tip point trajectory. Relaxing the requirement that tip orientation be tangent to path at each point greatly decreases both the base stroke and the pressure exerted on the tissue.

It may also be stressed that the ability to control the needle by its bending decreases deeper in the tissue and other techniques may be suggested.

We performed a qualitative experiment confirming the proposed concept. The needle trajectory was similar to the preplanned, avoiding an obstacle and hitting a target. Future research is focused on nonlinear beam approximation and close loop control utilizing an imaging system.

Acknowledgment. We thank Gábor Kósa and Micha Adler for their assistance with experiments.

References

1. De Andres J., Reina M.A., Lopez-Garcia A., Risks of regional anesthesia: Role of equipment - Needle design, catheters, VII Annual, European Society of Regional Anaesthesia Congress, Geneva Sept. 16 - 19, 1998
2. DiMaio S. P. and Salcudean S. E., Needle Insertion Modeling and Simulation, IEEE Transactions on Robotics and Automation: Special Issue on Medical Robotics, October 2003.
3. DiMaio S. P. and Salcudean S. E., Needle Steering and Model-Based Trajectory Planning, Proceedings of Medical Image Computing and Computer-Assisted Intervention, Montreal, 2003.
4. Alterovitz R., Pouliot J., Taschereau R., Hsu I. J., Goldberg K.. Sensorless Planning for Medical Needle Insertion Procedures. Proceedings of the 2003 IEEE/RSJ International Conference on Intelligent Robots and Systems (IROS 2003), October 2003
5. Chohan U, Hamdani G. A., Post Dural Puncture Headache, JPMA Vol:53, No.8 August 2003.
6. Mineta, T., Mitsui, T., Watanabe, Y., Kobayashi, S., Haga, Y., Esashi, M.: Batch fabricated flat meandering shape memory alloy actuator for active catheter. In: Sensors and Actuators A: Physical. Volume 88. (2001) 112–120
7. Kataoka, H., Washio, T., Audette, M., Mizuhara, K.: A Model for Relations between Needle Deflection, Force, and Thickness on Needle Penetration. In: Medical Image Computing and Computer Aided Intervention. (2001) 966–974
8. Simone C., Modeling of needle insertion forces for percutaneous therapies, M.Sc. Thesis, Johns Hopkins University, May 2002.
9. Fung Y.C., Biomechanics: Mechanics Properties of Living tissues, 2nd ed., New York: Springer-Verlag, 1993, pp.277.
10. Simaan, N., Gluzman, D., Shoham, M., “Design Considerations of New Six Degrees-Of-Freedom Parallel Robots.” IEEE International Conference on Robotics and Automation, 1998, Vol. 2, pp. 1327-1333.